S 5-4

# Inter-scale Observation and Process Optimization for Guanosine Fermentation

Ju Chu*, Si-Liang Zhang, and Ying-Ping Zhuang

*State Key Laboratory of Bioreactor Engineering, East China University of Science and Technology, Shanghai 200237, People's Republic of China*

## Abstract

Guanosine fermentation process can be well predicted and analyzed by the proposed state equations describing the dynamic change of a bioreactor. Pyruvate and alanine were found to be characteristically accumulated along with the decline of the guanosine formation rate during the mid-late phase of the process. The enzymological study of the main pathways in glucose catabolism and the quantitative stoichiometric calculation of metabolic flux distribution revealed that it was entirely attributed to the shift of metabolic flux from hexose monophosphate (HMP) pathway to glycolysis pathway. The process optimization by focusing on the restore of the shift of metabolic flux was conducted and the overcoming the decrease of oxygen uptake rate (OUR) was taken as the relevant factor of the trans-scale operation. As a result, the production of guanosinewas increased from 17 g/L to over 34 g/l.

**Keywords:** inter-scale; state prediction; guanosine fermentation; optimization; metabolic flux shift

## 1. Introduction[1-3)]

In industrialized production, large-scale production of a metabolic product can only be materialized in a bioreactor, and the alteration of microscopic reaction conditions in a cell can only be realized through modification of the size of apparatus or the operation conditions. However, variation in the size of apparatus or the operation condition may lead to different results, since it is an extremely complicated multi-scale system. Bioreactor process using living cells as the main body in a large-scale cultivation can be divided into three scales, i.e., molecular (genetic), cellular (metabolic) and bioreactor system (macroscopic) of network structures, showing an inter-dynamic relationship between these different scales and grave non-linearity features. Henceforth, it becomes a difficult problem to seek the optimization of a system by attempting to use only a static kinetic approach in a bioreactor.

The observation and control of a bioreaction system is mostly carried out at a bioreactor meso-scale, hence, the problem of inter-scale operation will occur when we deal with the control of a cellular metabolic

flux. Inter-scale operation is a difficult task, and the analysis of inter-scale problem often needs inter-discipline and inter-technical measures. When we want to control a phenomenon at certain scale, an operable approach at another scale is usually needed. Each application has its own special main-scale, but we have to rely on some other relative sub-scale observation to solve a problem and consider the situation synthetically. Accordingly, as for the theoretical and methodological studies of a bioreactor, we must not rest on the traditional concept, and should focus our study on the interdependency among various scales, so as to analyze a process feature of certain scale by observing the phenomenon at another scale. Guanosine production has been enhanced by gene engineering[4-7] and optimization of operation conditions[8-10]. In this paper, an inter-scale analysis method is proposed and applied to the optimization of guanosine fermentation successfully.

## 2. Materials and Methods

### 2.1 Microorganism and cultivation

Bacillus subtilis AJ2066 (Ade-) from Star Lake Bioscience Co., Inc. was cultured from a 8% (v/v) inoculum on medium composed of (g l-1) glucose 120, yeast extract 10, KH2PO4 5, (NH4)2SO4 15, MgSO4 2 and corn steep liquor 1 using a 50 l fermentor cultivated at 37 °C.

### 2.2 Fermentation system 2

Fermentation experiment was carried out in an automatic fermenter Model FUS-50A with online multi-parameter monitoring and control, including pH, dissolved oxygen (DO), back pressure (P), volume of fermentation broth (V), airflow rate (F), stirrer speed (RPM), ammonia concentration (ANH3.H2O), CO2 content in exhaust gas (ECO2), O2 content in exhaust gas (EO2), CO2 evolution rate (CER), O2 uptake rate(OUR), oxygen volumetric mass transfer coefficient (KLa) etc, and off-line manual determination of NH2-N, NH4+-N, glucose and guanosine.

### 2.3 Analysis

Growth was determined turbidimetrically at 650 nm (OD650). Glucose was measured with a glucose oxidase kit. Guanosine was measured by HPLC using a hypersil ODS C18 column (250 mm × 4 mm) with 0.5 % KH2PO4 solution as eluant at 1.2 ml min-1. The eluate was measured at 254 nm. Acetate, pyruvate and citric acid were measured by HPLC using a symmetry shield RP18 column (150 mm × 3.9 mm) with 0.01 mol l-1 H2SO4 as eluant at 1 ml min-1. The eluate was measured at 210 nm. Amino acids were measure by AccQ-Tag method.[8] NH2-N was measured by formaldehyde method. NH4+-N was measured by Kjeldahl method. O2 concentration of exhaust was measured with CY-101 magnetism pressure oxygen analysis instrument. CO2 concentration of exhaust was measured with GXH-101 infrared gas analysis instrument.

### 2.4 Determination of intracellular enzyme activity

Cell-free extract was prepared according to Fisher & Mangasanik[12] and kept at 4 °C, awaiting for the assay of intracellular enzyme activity. The enzymatic assays were performed for glucose kinase (GK, E.C.2.7.1.1),[13] phosphofructokinase (PFK, E.C.2.7.1.11),[14] pyruvate kinase (PYK, E.C.2.7.1.40),[15] L-alanine dehydrogenase (AlaDH, E.C.1.4.1.1),[16] citrate synthetase (E.C.4.1.3.7)[17] and 6-phosphoglucose dehydrogenase (G-6-PDH, E.C.1.1.1.49)[18] by using UNICO UV-2102PC spectrophotometer. Protein was measured by the Coomassie Brilliant Blue method.

## 3. Results and Discussions

### 3.1 Data acquisition in the course of guanosine fermentation

A typical time-course of multi-parameters profile obtained from repeated experiments was shown in Figure 1. It can be seen from the graphic presentation that during the late phase of fermentation, the production of guanosine declined evidently, while the glucose consumption rate still increased. Firstly, it can be derived from the carbon element balance that the intermediates were accumulated. Considering that the feeding of ammonia was increased synchronously at this time, this perhaps was due to the acid/base balance during the accumulation of organic acids (physical process), or the accumulation of nitrogenous organic intermediates mixture, which consumed nitrogen (biological process). If intermediary compounds, such as organic acids or amino acids accumulated, then the decline of OUR and CER suggesting that the shift of metabolic flux occurred.

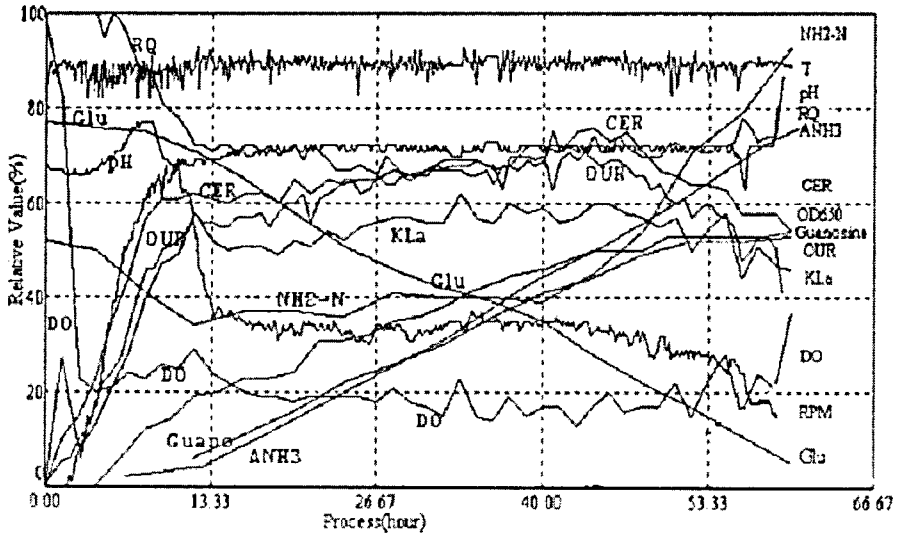


**Fig. 1 Typical data profiles during guanosine fermentation**

### 3.2 Establishment of a state equation and recognition of a system

In order to observe the unequilibrium phenomenon of substrate consumption and product formation further, a monitor was applied to estimate the status, i.e., on the basis of the estimation of environmental

variables(Evs) and physiological varaibles(PVs), the establishment of a state equation to describe the dynamic change of a bioreactor. In order to predict any unknown intermediate, the variables relevant to cell growth and metabolite balance were selected as a basis for the establishment of a state equation, combine the EVs and PVs vectors and set up a state equation for guanosine fermentation as follows:

$$\frac{dx}{dt}=\mu_m x(1-\frac{x}{x_m})+w_1$$

$$\frac{ds}{dt}=-Y_{S/x}\frac{dx}{dt}-m_1 x-Y_{S/P_1}\frac{dp}{dt}-Y_{S/P_2}\frac{dp}{dt}+w_2$$

$$\frac{dp_1}{dt}=\varphi_1 x+w_3$$

$$\frac{dp_2}{dt}=\varphi_2 x+w_4$$

$$\frac{dG_{CO_2}}{dt}=Y_{CO_2/x}\frac{dx}{dt}+m_2 x+Y_{CO_2/P_1}\frac{dp_1}{dt}+Y_{CO_2/P_2}\frac{dp_2}{dt}+w_5$$

$$\frac{dS_N}{dt}=-Y_{N/x}\frac{dx}{dt}-Y_{N/P_1}\frac{dp_1}{dt}-Y_{N/P_2}\frac{dp_2}{dt}+I_N+w_6$$

Since the parameters are changing as the process running, we can develop an extended state equation, taking the parameters as quasi-state quantity with noise, and apply the Extended Kalman Filter (EKF) theory for the estimation of both the parameter and the state. The extended state equation is as follows:

$$\frac{dx}{dt}=\mu_m x(1-\frac{x}{x_m})+w_1=f_1+w_1$$

$$\frac{ds}{dt}=-Y_{S/x}\frac{dx}{dt}-m_1 x-Y_{S/P_1}\frac{dp_1}{dt}-Y_{S/P_2}\frac{dp_2}{dt}+w_2=f_2+w_2$$

$$\frac{dp_1}{dt}=\varphi_1 x+w_3=f_3+w_3$$

$$\frac{dp_2}{dt}=\varphi_2 x+w_4=f_4+w_4$$

$$\frac{dG_{CO_2}}{dt}=Y_{CO_2/x}\frac{dx}{dt}+m_2 x+Y_{CO_2/P_1}\frac{dp_1}{dt}+Y_{CO_2/P_2}\frac{dp_2}{dt}+w_5=f_5+w_5$$

$$\frac{dS_N}{dt}=-Y_{N/x}\frac{dx}{dt}-Y_{N/P_1}\frac{dp_1}{dt}-Y_{N/P_2}\frac{dp_2}{dt}+I_N+w_6=f_6+w_6$$

$$\frac{d\mu_m}{dt}=0+w_7=f_7+w_7$$

$$\frac{dY_{N/P_2}}{dt}=0+w_{21}=f_{21}+w_{21}$$

The observation equation is as follows:

$$Z=HX+V.$$

$$H=\begin{bmatrix}1&0&0&0&0&0\\0&1&0&0&0&0\\0&0&1&0&0&0\\0&0&0&0&0&0\\0&0&0&0&1&0\\0&0&0&0&0&1\end{bmatrix}$$

$$X=[x_1 \quad x_2 \quad x_3 \quad x_4 \quad x_5 \quad x_6]^T$$

Filter was initiated at the inoculation, and the initial conditions were set as follows:

x(0) = 0.15815, S(0) =15.4, $P_1(0) = 0$, $P_2(0) = 0$, $G_{co2}(0) = 0$, $\mu_m(0)$ =0.0641, $x_m(0)$ =0.5376, $Y_{s/x}(0)$ = 4.9608, $m_1$=0.04995, $Y_{S/P_1}(0)$ =1, $Y_{S/P_2}(0)$=1, $Y_{co_2/x}(0)$=0.55222, $m_2$=0.001, $Y_{co_2/P_1}(0)$ = 0.38845, $Y_{co_2/P_2}(0)$=-0.61198, $\varphi_1$=0.78057

From the state estimation, it can be observed that around 40 h of fermentation P1 productivity $\varphi_1$ declined, and P2 productivity $\varphi_2$ gradually increased after 40 h of fermentation. Thus it can be seen that on the basis of the analytical studies above, and by estimating the state of the whole system, an unknown intermediates P2 was found to be generated around 40 h of fermentation, the result of which was shown in Figure 2.

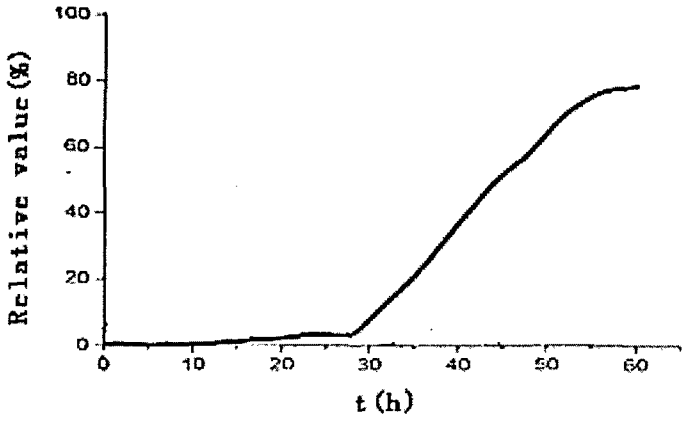


**Fig. 2 Estimated value of $P_2$ by EKF. — estimated value of unknown product P2**

### 3.3 Preliminary inference of the shift of metabolic flux

*3.3.1 Accumulation of organic acids*

The results of the analysis of organic acids (Fig 3) showed evidently that the pyruvate has been

characteristically accumulated, and at the same time the concentration of citric acid declined. In the entire process, acetate remained almost constant.

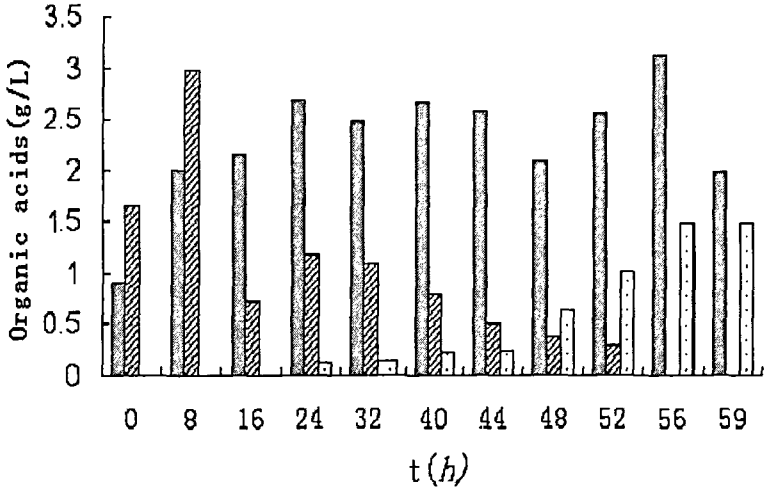


**Fig 3. Change of organic acids during guanosine fermentation process acetate(▩), citric acid(▨) and pyruvate(□)**

*3.3.2 Accumulation of amino acid*

The result of the analysis of amino acid components (Table 1) indicated that at the beginning of fermentation, glutamate concentration was rather high, and all the other amino acids were low. Along with

**Table 1. Time course of the changes of 17 amino acids in guanosine fermentation**

| Variety of amino | Amount of amino acid accumulation in broth (mmol/L) | | | | | | | | | |
|---|---|---|---|---|---|---|---|---|---|---|
| acid | 0(h) | 8(h) | 16(h) | 24(h) | 32(h) | 44(h) | 48(h) | 52(h) | 56(h) | 59 |
| Ala | 1.12 | 0.4 | 0.48 | 0.56 | 0.28 | 0.24 | 0.84 | 6.8 | 14.2 | 13.84 |
| Arg | 0.16 | ND | ND | ND | ND | ND | ND | ND | 0.6 | 1.32 |
| Asp | 0.2 | ND | ND | ND | ND | ND | ND | ND | ND | ND |
| Cys2 | 0.04 | 0.04 | 0.04 | 0.08 | 0.04 | 0.04 | 0.04 | 0.08 | 0.32 | 0.28 |
| Glu | 16.28 | 1.84 | ND | ND | ND | ND | ND | 0.12 | 0.08 | 0.08 |
| Gly | 0.28 | ND | ND | ND | ND | ND | ND | ND | 0.08 | 0.08 |
| His | ND | ND | ND | ND | ND | ND | ND | ND | ND | ND |
| ILe | 0.16 | ND | 0.24 | ND | ND | ND | ND | ND | 0.08 | 0.12 |
| Leu | 0.4 | ND | 0.08 | 0.08 | ND | ND | ND | 0.04 | ND | ND |
| Lys | 0.28 | ND | ND | 0.36 | 0.28 | 0.08 | 0.12 | 0.32 | 0.4 | 0.36 |
| Met | 0.08 | 0.4 | 0.64 | 0.08 | 0.04 | ND | ND | 0.08 | 0.2 | 0.2 |
| Phe | 0.16 | ND | 0.16 | 0.36 | 0.36 | 0.4 | 0.36 | 0.64 | 0.4 | 0.32 |
| Pro | 0.36 | 0.32 | 0.28 | 0.52 | 0.36 | 0.12 | 0.2 | 0.2 | 0.88 | 0.8 |
| Ser | 0.32 | ND | ND | ND | ND | ND | ND | ND | 0.12 | 0.12 |
| Thr | 0.2 | 0.04 | ND | ND | 0.08 | ND | 0.12 | 0.08 | 1.52 | 1.68 |
| Try | 0.2 | ND | ND | 1.24 | 0.28 | 1.2 | 1.04 | 1.52 | 1.44 | 1.2 |
| Val | 0.32 | 0.12 | 0.72 | 0.56 | 0.24 | 0.28 | 0.2 | 0.36 | 0.6 | 0.56 |
| Total | 20.56 | 3.16 | 2.64 | 3.84 | 1.96 | 2.36 | 2.92 | 10.24 | 20.92 | 20.96 |

the fermentation glutamate was quickly assimilated for cell synthesis, and declined to a very low level at 8 h of fermentation, and maintained at this level till the end of fermentation. The accumulation of alanine became apparent at around 40 h of fermentation, the amount accumulated was 12.6 times as the initial level, and the other 16 amino acids were almost unchanged, and kept at rather low level till the end of fermentation.

*3.3.3 association analysis of organic acids and amino acids*

It can be seen, from the time sequencing changes of amino acids and organic acids during fermentation, that the accumulation of amino acids was mainly alanine, and its accumulation was later than that of organic acids and [$NH_4^+$]. The result was coincident with Figure 2. Hence, it should be attributed to the shift of metabolic flux, which was caused by the transfer of metabolic pathway. Since the synthesis of alanine can be converted immediately from pyruvate, it is intelligible that the increase of EMP flux led to the accumulation of pyruvate, and subsequently converted to alanine. Alanine itself could inhibit and repress the synthesis of glutamine synthetase, which resulted in the reduction of HMP flux, and subsequent production of guanosine.

**3.4 Improvement of guanosine fermentation and process optimization**

According to the above results, process optimization was carried out by focusing on the restore of the shift of metabolic flux from EMP to HMP pathway, and taking the decrease of OUR as the relevant factor of the trans-scale operation. It was found that the decrease rate of OUR became alleviated soon after the addition of the regulation factor A in the mid-late phase of fermentation, and kept constant from 48 h to the end of fermentation, and the consumption rate of glucose became retarded during late phase of fermentation. The production of guanosine was increased from 17 g $l^{-1}$ to 34 g $l^{-1}$. The changes of the concentration of alanine and pyruvic acid after adopting the new regulatory technology were shown in Fig.4.

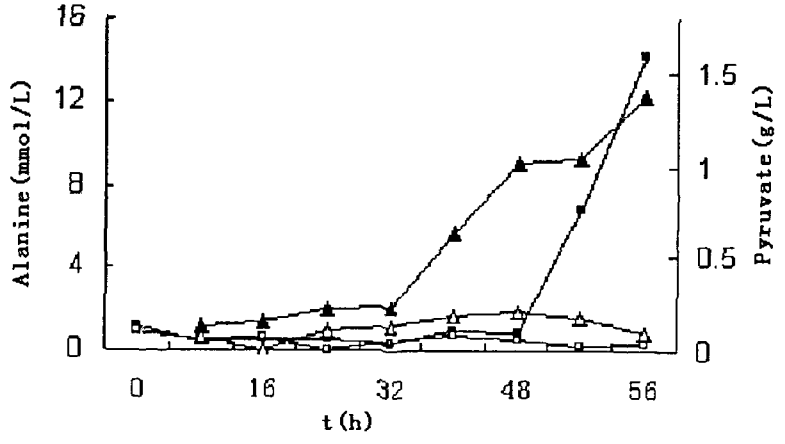


**Fig. 4 Time courses of accumulation of alanine and pyruvate for use of two technologies**
alanine with original(—□—) and alanine with new technology(—■—), pyruvate with original(—△—) and pyruvate with new technology (—▲—)

### 3.5 Study of the metabolic flux using stoichiometry

*3.5.1 Construction of metabolic network*[19,20]

The metabolic network of *B. subtilis* was simplified as shown in Figure 5. The metabolic network is comprised of 5 parts: EMP and HMP pathway, TCA cycle, oxidative phosphorylation and the accumulation of metabolites. Table 2 showed the metabolic equations of the metabolic network and Table 3 listed the equation set taking the element balance and the metabolic network of cell growth into account synthetically.

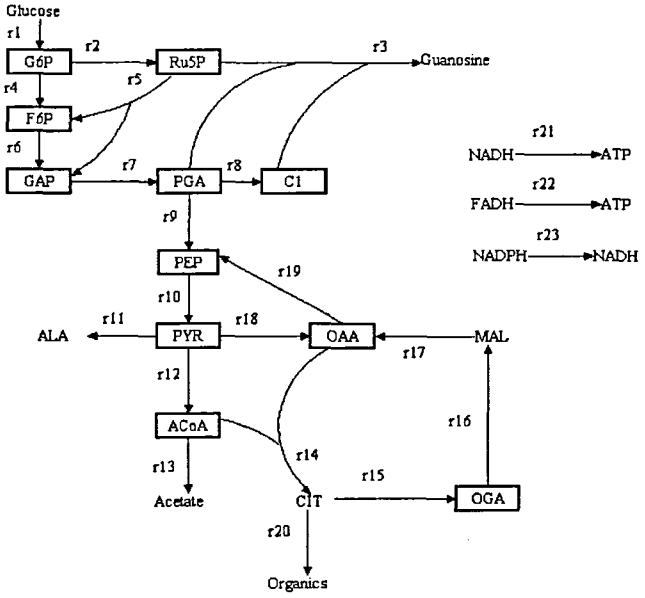


**Fig. 5 Metabolic equations of the metabolic network.**

**Table. 2 The metabolic reactions of *B. subtilis***

$r_1$ : Glucose $\longrightarrow$ G6P

$r_2$ : G6P $\longrightarrow$ Ru5P + 2NADPH + $CO_2$

$r_3$ : Ru5P + PGA + C1 + $CO_2$ + 11ATP + 2NADPH $\longrightarrow$ Guanosine + 3NADH

$r_4$ : G6P $\longrightarrow$ F6P

$r_5$ : Ru5P $\longrightarrow \frac{2}{3}$ F6P + $\frac{1}{3}$ GA *P*

$r_6$ : F6P + ATP $\longrightarrow$ 2GAP

$r_7$ : GAP $\longrightarrow$ PGA + ATP + NADH

$r_8$ : PGA + NADPH $\longrightarrow$ 2C1 + $CO_2$ + NADH

$r_9$ : PGA $\longrightarrow$ PEP

$r_{10}$ : PEP $\longrightarrow$ PYR + ATP

$r_{11}$ : PYR + NADPH $\longrightarrow$ ALA

$r_{12}$ : PYR $\longrightarrow$ ACoA + NADH + $CO_2$

$r_{13}$ : ACoA $\longrightarrow$ Acetate + ATP

$r_{14}$ : ACoA + OAA $\longrightarrow$ CIT

$r_{15}$ : CIT $\longrightarrow$ OGA + NADPH + $CO_2$

$r_{16}$ : OGA $\longrightarrow$ MAL + NADH + FADH + ATP + $CO_2$

$r_{17}$ : MAL $\longrightarrow$ OAA + NADH

$r_{18}$ : PYR + $CO_2$ + ATP $\longrightarrow$ OAA

$r_{19}$ : OAA + ATP $\longrightarrow$ PEP + $CO_2$

$r_{20}$ : CIT $\longrightarrow$ Organics

$r_{21}$ : NADH + $\frac{1}{2}O_2 \longrightarrow$ 1.3 ATP

$r_{22}$ : FADH + $\frac{1}{2}O_2 \longrightarrow \frac{2}{3}$ (1.3 ATP)

$r_{23}$ : NADPH $\longrightarrow$ NADH

**Table. 3 The metabolic equation set of *B. subtilis***

$x_1(\text{Glucose}): -r_1 = q_{\text{Glucose}}$

$x_2(\text{G6P}): r_1 - r_2 - r_4 = 154 \times 10^{-6}\mu$

$x_3(\text{F6P}): r_4 + \frac{2}{3}r_5 - r_6 = 190 \times 10^{-6}\mu$

$x_4(\text{Ru5P}): r_2 - r_3 - r_5 = (816 + 308) \times 10^{-6}\mu$

$x_5(\text{Guanosine}): r_3 = q_{\text{Guanosine}}$

$x_6(\text{GAP}): \frac{1}{3}r_5 + 2r_6 - r_7 = 194 \times 10^{-6}\mu$

$x_7(\text{PGA}): -r_3 + r_7 - r_8 - r_9 = 1395 \times 10^{-6}\mu$

$x_8(\text{C1}): -r_3 + 2r_8 = 156 \times 10^{-6}\mu$

$x_9(\text{PEP}): r_9 - r_{10} + r_{19} = 711 \times 10^{-6}\mu$

$x_{10}(\text{PYR}): r_{10} - r_{11} - r_{12} - r_{18} = 2942 \times 10^{-6}\mu + q_{\text{PYR}}$

$x_{11}(\text{ALA}): r_{11} = q_{\text{ALA}}$

$x_{12}(\text{ACoA}): r_{12} - r_{13} - r_{14} = 2132 \times 10^{-6}\mu$

$x_{13}(\text{Acetate}): r_{13} = q_{\text{Acetate}}$

$x_{14}(\text{OAA}): -r_{14} + r_{17} + r_{18} - r_{19} = 1923 \times 10^{-6}\mu$

$x_{15}(\text{CIT}): r_{14} - r_{15} - r_{20} = q_{\text{CIT}}$

$x_{16}(\text{OGA}): r_{15} - r_{16} = 1071 \times 10^{-6}\mu$

$x_{17}(\text{MAL}): r_{16} - r_{17} = 0$

$x_{18}(\text{CO}_2): r_2 - r_3 + r_8 + r_{12} + r_{15} + r_{16} - r_{18} + r_{19} = -2052 \times 10^{-6}\mu + q_{\text{CO}_2}$

$x_{19}(\text{O}_2): -r_{21} - r_{22} = -2q_{\text{O}_2}$

$x_{20}(\text{NADPH}): 2r_2 - 2r_3 - r_8 + r_{15} - r_{23} = 16333 \times 10^{-6}\mu$

$x_{21}(\text{NADH}): 3r_3 + r_7 + r_8 + r_{12} + r_{16} + r_{17} - r_{21} + r_{23} = -3595 \times 10^{-6}\mu$

$x_{22}(\text{FADH}): r_{16} - r_{22} = 0$

$x_{23}(\text{Organics}): r_{20} = q_{\text{Organics}}$

*3.5.2 Results of calculation*

Making use of MATLAB language, the metabolic equation set under various operation conditions were

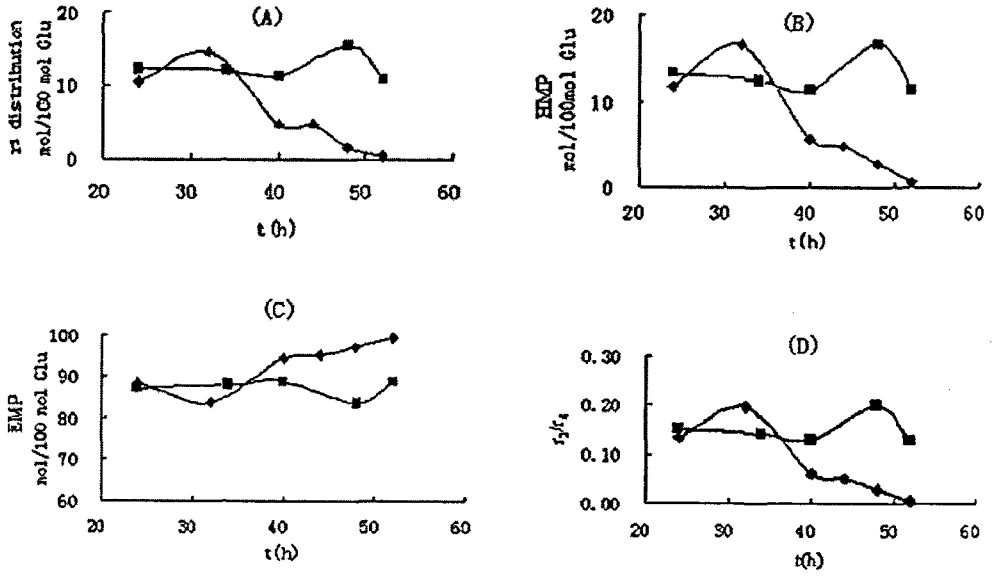


**Fig. 6 Flux distributions between two technologies with original ( —◆— ) and new technology ( —■— )**

programmed and solved. Figure 6 shows the changes in the flow rates of *r*2, *r*3, and *r*4 in different periods before and after improvement of the technology. It can be seen that the amount of F6P generated after 52 h of fermentation from the original and new technologies were 99 and 89 mol/100 mol glucose, respectively. Only 1 mol Ru5P/100 mol glucose was formed in the original process whereas 11 mol Ru5P/100 mol glucose was produced in the optimized process; this means the flux entering the HMP pathway was almost 10 times that of the original process.

### 3.6 Enzymological evidence for the shift of metabolic flux

Study of the dynamic activities of enzymes, which is related to the flux of these pathways, is useful for understanding the process and its optimization. Figure 7 showed the dynamic profiles of the activity of key enzymes during fermentation. The results showed that the decline of the rate of guanosine synthesis in the late phase could be attributed to metabolic flux shift to the EMP pathway. It was revealed that an "overflow" phenomenon occurred in the EMP pathway and in the TCA cycle, i.e. the activity of alanine dehydrogenase was increased apparently during the late phase of the process and strengthened the enzymatic capacity to convert pyruvate to alanine. The results clearly demonstrated the roles of the time-varying enzymes in regulating metabolism on the cellular scale, and presented immediate evidence of the metabolic flux shift.

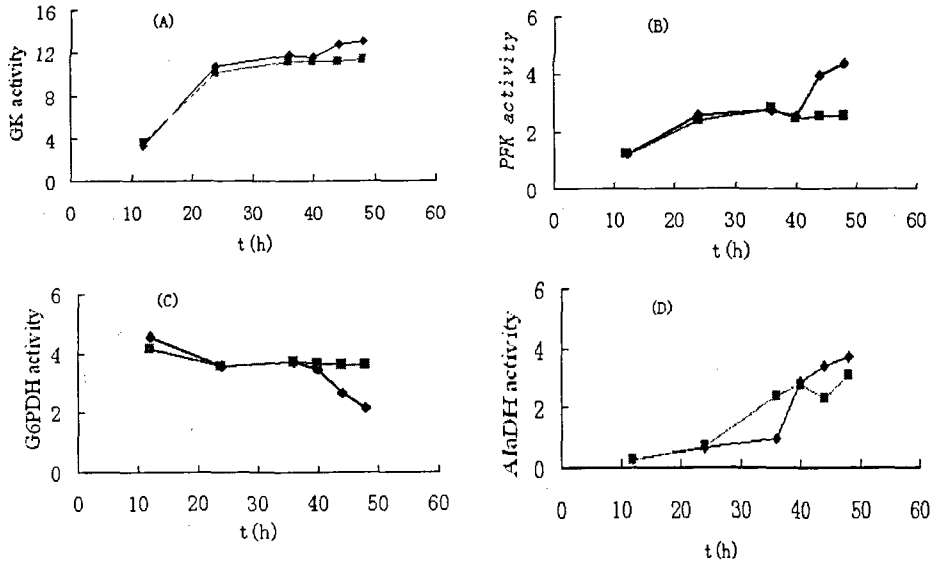


**Fig. 7 Time courses of various enzyme activities during fermentation original ( —◆— ) and new technology ( —■— )**

## 4. Conclusions

This study was carried out from the industrialization point of view. Making use of various means of monitoring and data processing by PC in a bioreactor, it was revealed that the shift of metabolic flux was

the key point of guanosine fermentation optimization. From the variation of the levels of amino acids and organic acids with time during the fermentation, it was easy to understand that accumulation of pyruvate, caused by the increase in EMP flux, has resulted in the formation of alanine, which was the feedback inhibitor of GS. This inhibition, in turn, led to a further decrease of HMP flux, which eventually caused a decrease in guanosine production rate. Besides, the results of gene sequence analysis of the guanosine producer strains showed that the frame shift mutation of the gene encoded for sAMP synthesis enzyme corresponding to high yield strain was disclosed, and partial promotor of its pur operon has undergone a variety of mutations, which was favorable to the production of guanosine. The results showed that the strain used for guanosine production has already possessed good hereditary potential and would not be a bottleneck for optimization of guanosine production.[21)]

The approach of inter-scale observation and process optimization was successfully applied to the guanosine fermentation. It can reflect the essence and highlight the intrinsic rule of a complicated process, while does not increase too much complexity and it is suitable for the practical engineering application.

## References


1. Zhang S-L,Chu J, and Zhuang Y-P A multi-scale study of industrial fermentation processe and their optimization, Adv Biochem Engin/Biotechnol, Springer-Verlag Berlin Heidelberg (2004).
2. Zhang S-L, Study on the fermentationprocess at multi-levels and bioreactor design and its application for special purposes. Engineering Science 8:37-44 (2001).
3. Zhang S-L, Zhang X-C, Zhao Y, Zhu Y-H and Lu R-L, Research on the production control of microbial secondary metabolism. Proceedings of the first national symposium on modeling and control of biotechnical processes, East China University of Chemical Technology Press, Shanghai (1989).
4. Ajinomoto Co., Inc., Guanosine production by Bacillus. JP58175493 (1983).
5. Miyagawa K, Nakahama K and Kikuchi M, Recombinant plasmids for guanosine production in *Bacillus subtilis*. EP151341 (1985).
6. Miyagawa K, Kimura H and Nakahama K, Cloning of the Bacillus subtilis IMP dehydrogenase gene and its application to increased production of guanosine. *BioTechnolog* 4:225-228 (1986).
7. Miyagawa K, Kanzaki N and Sumino Y, Enhanced manufacture of inosine and guanosine with recombinant *Bacillu*. EP286303 (1988).
8. Sumino Y, Sonoi K and Doi M, Manufacture guanosine by fermentation. GB2101131 (1983).
9. Tang S-R, Wang J-Y, Liu Z-H, Zhu X-W and Ju N-H, Improvement of guanosine yield by fed-batch culture. *Ind Microbio* 22:5-10 (1992).
10. Tang S-R, Huang W-H and Hou Z-R, Process of guanosine production by fermentation. *Ind Microbio* 28:11-16 (1998)
11. Lee K, Lee J, Kim YH, Moon SH and Park YH, Unique properties of four Lactobacilli in amino acid production and symbiotic mixed culture for lactic acid biosynthesis. *Curr Microbiol* 43 83-390 (2001).
12. Fisher SH and Mangasanik B, Synthesis of oxaloacetate in Bacillus subtilis mutants lacking the

2-ketoglutarate dehydrogenase enzymatic complex *J Bacteriol* 158:55-62 (1984).

13. Postma E, Scheffers WA and van Dijken JP, Adaptation of the kinetics of glucose transport to environmental conditions in the yeast Candida utilis CBS 621' continuous-culture study. *J Gen Microbiol* 134:1109-1116 (1988).
14. Alves AM, Euverink GJ, Bibb MJ and Dijkhuizen L, Identification of ATP-dependent phosphofructokinase as a regulatory step in the glycolytic pathway of the Actinomycete streptomyces coelicolor A3 (2). *Appl Environ Microbiol* 63 956-961(1997).
15. Malcovati M and Valentini G, AMP and fructose 6-phophate activated pyruvate kinase from *E.col. Methods Enzymol* 90:170-179 (1982).
16. Siranosian M, Alanine dehydrogenase is required for normal sporulation in *Bacillus subtilis*. J Bacteriol 15:6789-6796 (1993)
17. Fortnagel P and Freese E, Analysis of sporulation mutants II. Mutants blocked in the citric acid cycle. *J Bacteriol* 95:1434-1438 (1968)
18. Horne R, Anderson W and Nordlie R, Glucose dehydrogenase activity of yeast glucose-6-phosphate dehydrogenase. Inhibition by adenosine 5'-triphosphate and other nucleoside 5'-triphosphates and diphosphate. *Biochemistry* 9:610-615 (1970).
19. Sauer U, Cameron DC and Bailey JE, Metabolic capacity of Bacillu subtili for the production of purine nucleosid, riboflavin, and folic acid. *Biotechnol Bioeng* 59:227-238 (1998).
20. Goel A, Ferrance J, Jeong J and ataai MM, Analysis of Metabolic Fluxes in Batch and Continuous Cultures of *Bacillus subtilis. Biotechnol Bioeng* 42:686-696 (1993)
21. Qian J-C, Cai X-P, Chu J, Zhuang Y-P and Zhang S-L, Analysis of three nucleotide sequences involved in the purine nucleotides biosynthesis in inosine and guanosine-producing *Bacillus subtilis. Acta Microbiologica Sinica* 43:200-205 (2003)